

Image Cover Sheet

CLASSIFICATION

UNCLASSIFIED

SYSTEM NUMBER

148560

**TITLE**

THE DESIGN, MANUFACTURE AND PACKAGING OF AN ANAMORPHIC BEAM-EXPANDER TO
ILLUMINATE BRAGG CELLS IN A TIME-INTEGRATING CORRELATOR

System Number:**Patron Number:****Requester:****Notes:****DSIS Use only:****Deliver to:**

93-609

The design, manufacture and packaging of an
anamorphic beam-expander to illuminate Bragg
cells in a time-integrating correlator

Interim report submitted to

Defence Research Establishment
Department of National Defence
3701 Carling Ave.
Ottawa, Ontario
K1A 0K2

u/u/aci

by:

LASIRIS INC.
3549 Ashby
St-Laurent, Québec
H4R 2K3

LASIRIS

January 31, 1993

The design, manufacture and packaging of an
anamorphic beam-expander to illuminate Bragg
cells in a time-integrating correlator

Interim report submitted to

Defence Research Establishment
Department of National Defence
3701 Carling Ave.
Ottawa, Ontario
K1A 0K2

by:

LASIRIS INC.
3549 Ashby
St-Laurent, Québec
H4R 2K3

The logo for LASIRIS INC. features the word "LASIRIS" in a bold, sans-serif font. The letter "A" is replaced by a stylized graphic of a triangle with horizontal lines inside, suggesting a beam or a lens.

January 31, 1993

TABLE OF CONTENTS

INTRODUCTION	1
1. DESIGN AND CALCULATION OF AN ANAMORPHIC BEAM-EXPANDER BASED ON AN ASPHERICAL LENS	2
1.1 Basic considerations	2
1.2 Design and calculation	4
1.3 Characteristics of the best design	21
2. DESIGN OF AN ANAMORPHIC BEAM-EXPANDER BASED ON A HOLOGRAPHIC OPTICAL ELEMENT (HOE)	24
2.1 In-line geometry	24
2.2 Off-axis geometry	26
3. DESIGN OF AN ANAMORPHIC BEAM-EXPANDER BASED ON A DIFFRACTIVE ELEMENT	28
4. SELECTION OF THE BEST DESIGN	29

INTRODUCTION

As was described in our proposal for contract # W7714-2-9654/01-ST, the purpose of this project is to design and produce an anamorphic beam-expander to illuminate Bragg cells in a time-integrating correlator. The basic element of the beam-expander is a "Powell lens" (designed in 1987 by Ian Powell from the National Council of Research of Canada) which is an aspherical element capable of producing a beam with a uniform intensity diverging in one dimension on the X axis. On the other axis, Y, the size of the beam is determined only by the divergence of the laser beam. Unfortunately, the wavefront is not flat because of the presence of aberrations introduced by the lens itself. Our goal is to design and manufacture an element which would collimate the diverging beam exiting from a Powell lens, and correct the wavefront in order to obtain the best flatness possible, while still retaining the uniform intensity, on the X axis, of the beam.

The project is separated in two phases:

Phase 1 where the design and calculation of an anamorphic beam-expander based on three different elements are performed, and Phase 2 where the prototype beam-expander is manufactured and packaged according to the selected design.

This preliminary report illustrates the work done under Phase 1 and is divided in four chapters describing respectively:

- 1- Correction of the wavefront emerging from a Powell lens by an aspherical lens
- 2- Correction of the wavefront emerging from a Powell lens by a holographic optical element (HOE)
- 3- Correction of the wavefront emerging from a Powell lens by a glass diffractive element
- 4- Selection of the best design.

1. DESIGN AND CALCULATION OF AN ANAMORPHIC BEAM-EXPANDER BASED ON AN ASPHERICAL LENS

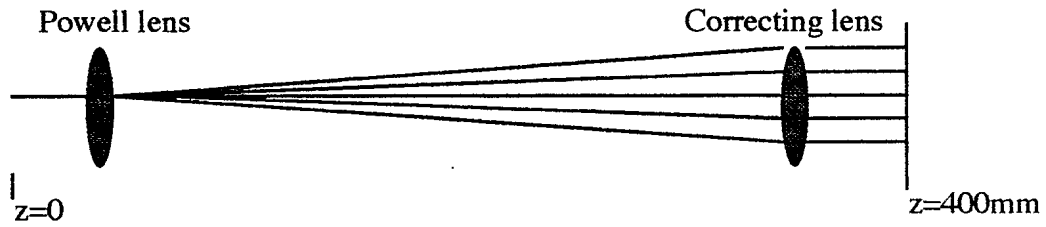
1.1 Basic considerations

The first elements that were considered before working on the design of the beam-expander were the following required final parameters:

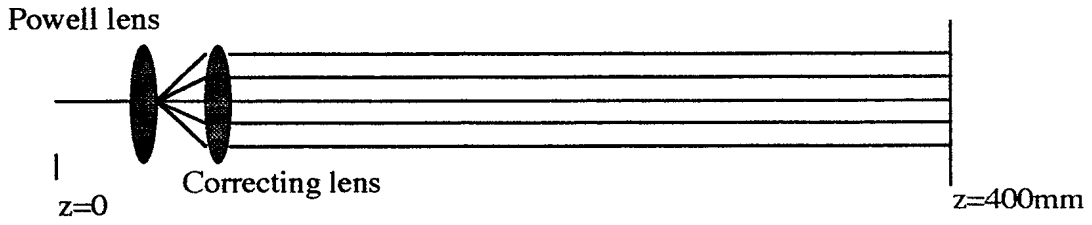
- | | |
|--|---|
| 1. Length of the expanded beam: | 35 mm, the source of illumination being a He-Ne laser with a .68 mm beamwaist and a 1.2 mrad divergence. |
| 2. Maximum size of the packaged beam expander: | width: 10 cm
length: 45 cm
height: 10 cm
with the optical axis at a height between 5 cm and 6 cm from the optical table. |
| 3. Uniformity of the wavefront of the expanded beam: | $\lambda / 10$ |
| 4. Uniformity of the intensity on the X axis: | Fluctuations at any point of the distribution are not to be more than 10 % of the average value of the intensity of the illumination. |

The first two requirements were relatively easy to attain while the third and fourth were the goals to be reached or approached. Consequently, each design has been evaluated and improved according to requirements 3 and 4.

Figure 1 displays the extreme design geometries to consider if the wavefront final plane is put arbitrarily at $z = 400$ mm. A compromise must be found between the two depicted situations. In figure 1.a the small divergence of the Powell lens minimizes the aberrations and makes the requirement of a flat wavefront likely to be satisfied, but the intensity distribution of the resulting laser line may not be uniform. On the other hand, in figure 1.b the high divergence of the Powell lens is likely to transform the laser gaussian intensity distribution into a uniform one, but the strong aberrations introduced in the wavefront will be quite impossible to correct with a single element.



a. Longest geometry, smallest divergence of Powell lens.



b. Shortest geometry, highest divergence of Powell lens.

Figure 1. Extreme design geometries

1.2 Design and calculation

Optimization of the designs and calculation of the lenses profile were performed using a computer program called "BEAM THREE OPTICAL RAY TRACER" from Stellar Software. The iterative calculations were made according to the following method: the vertex of the Powell lens was arbitrarily put at $z = 15$ mm and the wavefront observation plane at $z = 400$ mm. For simplicity the thickness and the diameter of the Powell lens were fixed to 9 mm, the thickness of the correcting lens to 9 mm and its height to 45 mm (along the X axis). A certain geometry was chosen (short or long) and the radius and conic constant of the aspherical surface of the Powell lens were optimized to produce the required divergence of the beam. Thereafter the vertex position of the correcting lens was fixed where the beam diameter was 35 mm and the radius and conic constant of its aspherical surface were optimized to produce a collimated emerging beam. Finally a spot diagram of the rays optical pathlength was traced at the observation plane and the intensity distribution of the line projected on the observation plane was calculated. The whole process was applied again for another geometry and the final results were compared.

Table 1 shows a summary of the final results related to the four most representative geometries that were calculated.

Geometry		Intensity distribution	Wavefront flatness
1	6° fan angle	Min intensity=.5 Max intensity over 28 mm	.25 to .5 λ over 35 mm
	36 cm beam-expander	Min intensity=.2 Max intensity over 35 mm	.1 λ over 16 mm
2	12° fan angle	Intensity= $\pm 10\%$ aver. intensity over 30 mm	.5 to .8 λ over 35 mm
	20 cm beam-expander	Min intensity=.7 Max intensity over 35 mm	.1 λ over 5 mm
3	12° fan angle	Intensity= $\pm 10\%$ aver. intensity over 28 mm	.5 to 1 λ over 34 mm
	19 cm beam-expander	Min intensity=.3 Max intensity over 35 mm	.1 λ over 5.6 mm
4	30° fan angle		2 to 2.5 λ over 35 mm
	10 cm beam-expander	Intensity= $\pm 20\%$ aver. intensity over 35 mm	

Table 1. Comparative results of four selected geometries

It can be seen that the second geometry, with the 12° Powell lens fan angle, gives the overall best results. The difference between the second and third geometries is that in the second one, the length of the beam-expander is made slightly longer so the projected laser line is 37 mm long instead of 35 mm and consequently the intensity distribution and the wavefront flatness are improved over 35 mm. The results indicate that a compromise must be done between the intensity distribution uniformity and the wavefront flatness. A geometry that makes a noticeable gain in one makes a degradation in the other.

To calculate the wavefront flatness it was necessary to simulate a ray trace of the laser beam through the different optical elements. Since our computer ray tracer only deals with geometrical optics, we had to "imitate" the laser beam divergence by giving the 1000 random rays the possibility to have an initial angle of incidence as measured from the optical axis. This method gave the upper limit of the wavefront flatness interval given in table 1. The lower limit was found by giving the rays a null initial angle of incidence.

Table 2 gives the principal parameters related to the design of the four beam-expanders of table 1. Column 2 shows the position on the Z axis of each surface of the two lenses in the beam-expanders, while columns 3 and 4 display the curvature C (inverse radius) and the conic constant Q of each surface profile.

Geometry	Z (mm)	C (mm ⁻¹)	Q	Index	surface #
1 6° fan angle	15	0.3500	-19.0	BK7	1
	24	0.0			2
	353.20	0.0		BK7	3
	362.20	-0.0058	-0.24	BK7	4
2 12° fan angle	15	0.9221	-13.0	BK7	1
	24	0.0			2
	190.45	0.0		BK7	3
	199.45	-0.0110	-0.22	BK7	4
3 12° fan angle	15	0.9524	-15.0	BK7	1
	24	0.0			2
	181.22	0.0		BK7	3
	190.22	-0.0116	-0.14	BK7	4
4 30° fan angle	15	2.3810	-3.5	BK7	1
	24	0.0			2
	87.76	0.0		BK7	3
	96.76	-0.0259	-0.48	BK7	4

Table 2. Optical parameters for the beam-expanders

Figures 2 to 5 show an outline of the four beam-expander designs according to geometries 1 to 4. Figure 6 displays a spot diagram of the line generated by those beam-expanders, while figure 7 sketches a spot diagram of the pathlength of the rays, at the entrance plane of the correcting lens, for geometry #2 which proved to be the best. It can be seen that the wavefront flatness is in the order of $10^4 \lambda$. By comparison, figures 8 to 11 display the same spot diagram traced at the observation plane ($z = 400$ mm), after passing through the correcting lenses of geometries 1 to 4. It is obvious that in all cases the wavefront flatness is greatly improved. These diagrams present a spreading of the spots, due to the fact that the 1000 random rays were allowed to have a varying initial angle of incidence. Thus the diagrams give the upper limit of the wavefront flatness. One can observe that the "longer" the geometry, the better the wavefront flatness.

Figures 12 to 15 display the intensity distribution of the lines generated by the 4 beam-expanders at the observation plane $z = 400$ mm. Results are given for half the length of the lines, but it is understood that the intensity distribution is symmetrical on the other half. Calculations have been performed using a simple technique: at the observation plane we consider a column of boxes placed at every two millimeters, we trace 2000 random rays and count the number of rays collected by each box. The intensity distribution is then given by the percentage of collected rays in each box as a function of the box position. The dashed line on the graphs gives the resulting intensity distribution when the source of illumination has a uniform intensity distribution, and the solid line gives the resulting distribution for a source with a gaussian intensity distribution (which was simulated by weighing the rays according to a gaussian apodization function across the aperture) . It can be seen that the most uniform intensity distribution over 17.5 mm is for geometry # 2.

1-D telescope with first lens fan-angle of 6 degrees

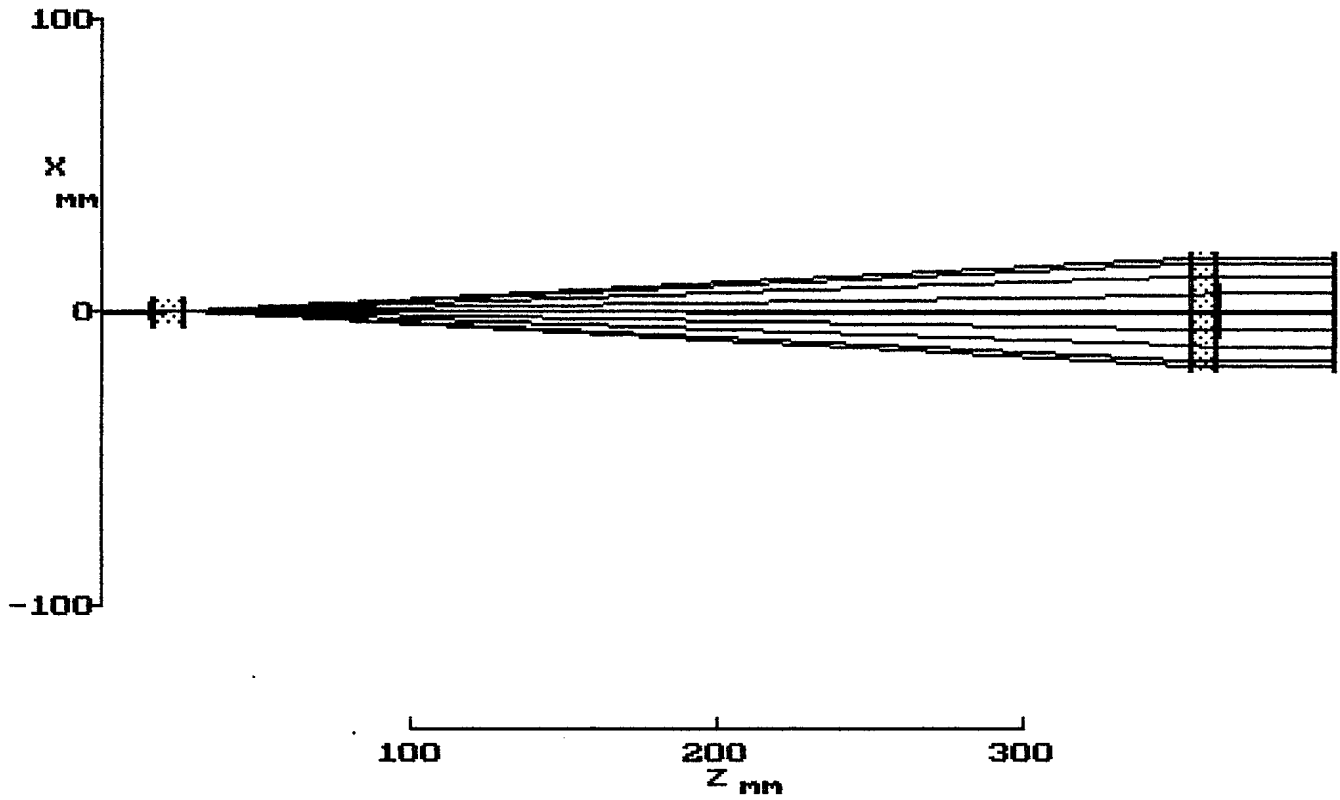


Figure 2. Outline of the beam-expander design, geometry #1

1-D telescope with first lens fan-angle of 12 degrees
(longer geometry)

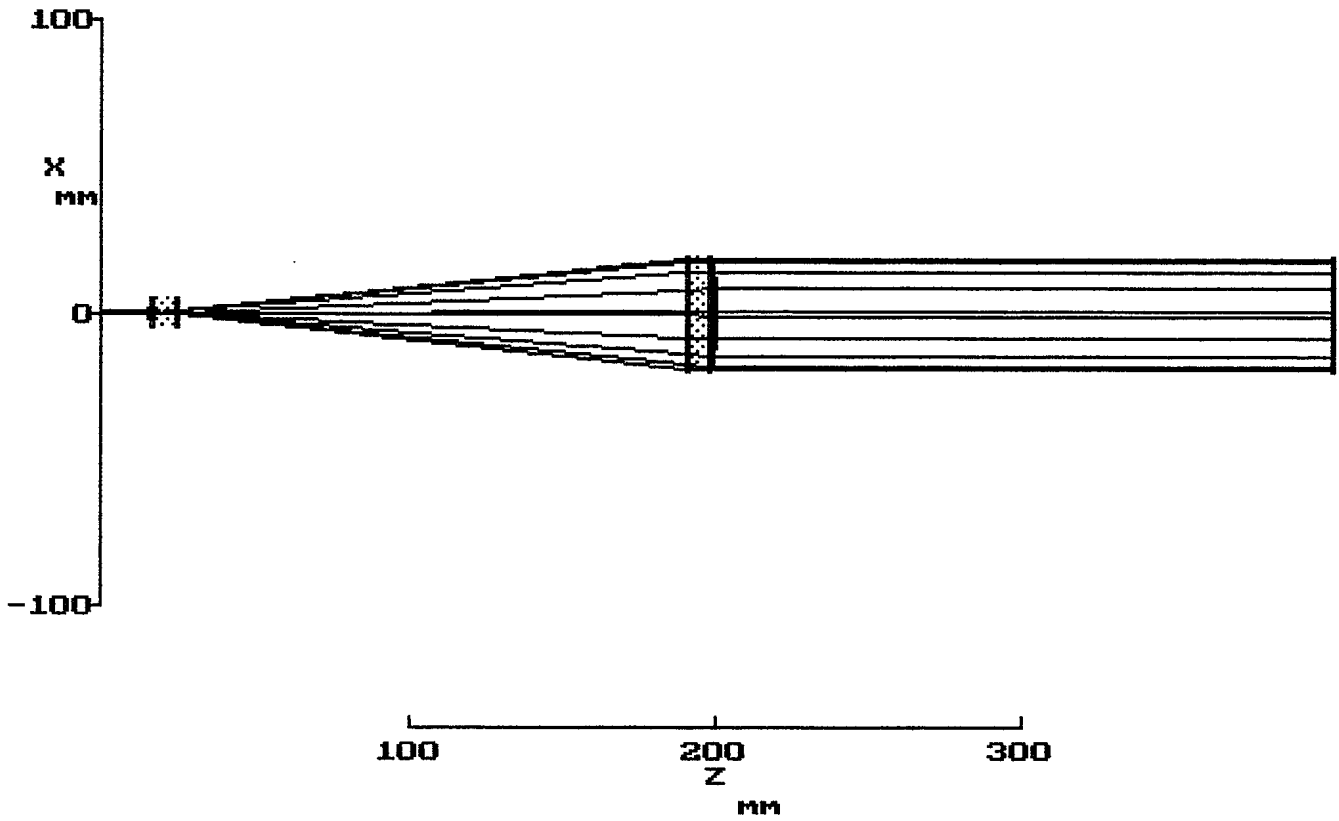


Figure 3. Outline of the beam-expander design, geometry #2

1-D telescope with first lens fan-angle of 12 degrees

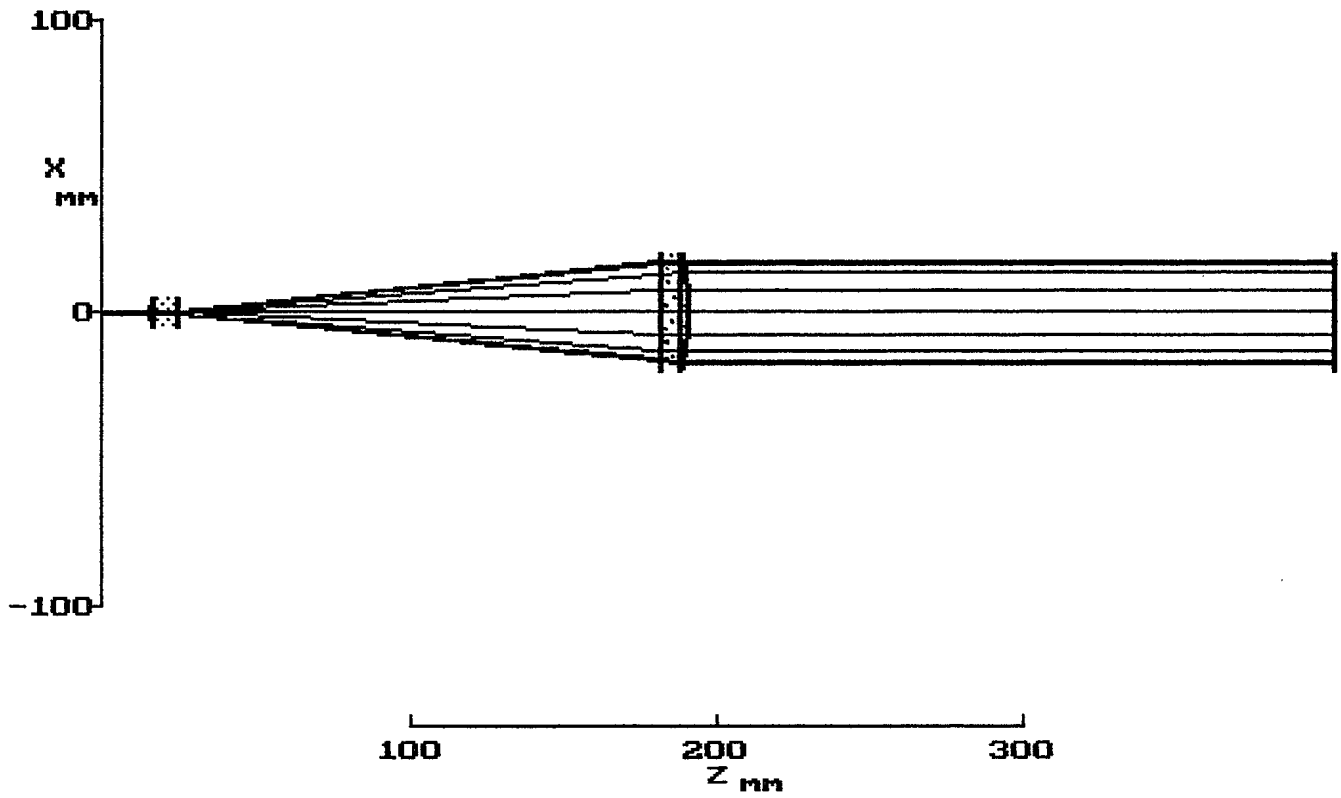


Figure 4. Outline of the beam-expander design, geometry #3

1-D telescope with first lens fan-angle of 30 degrees

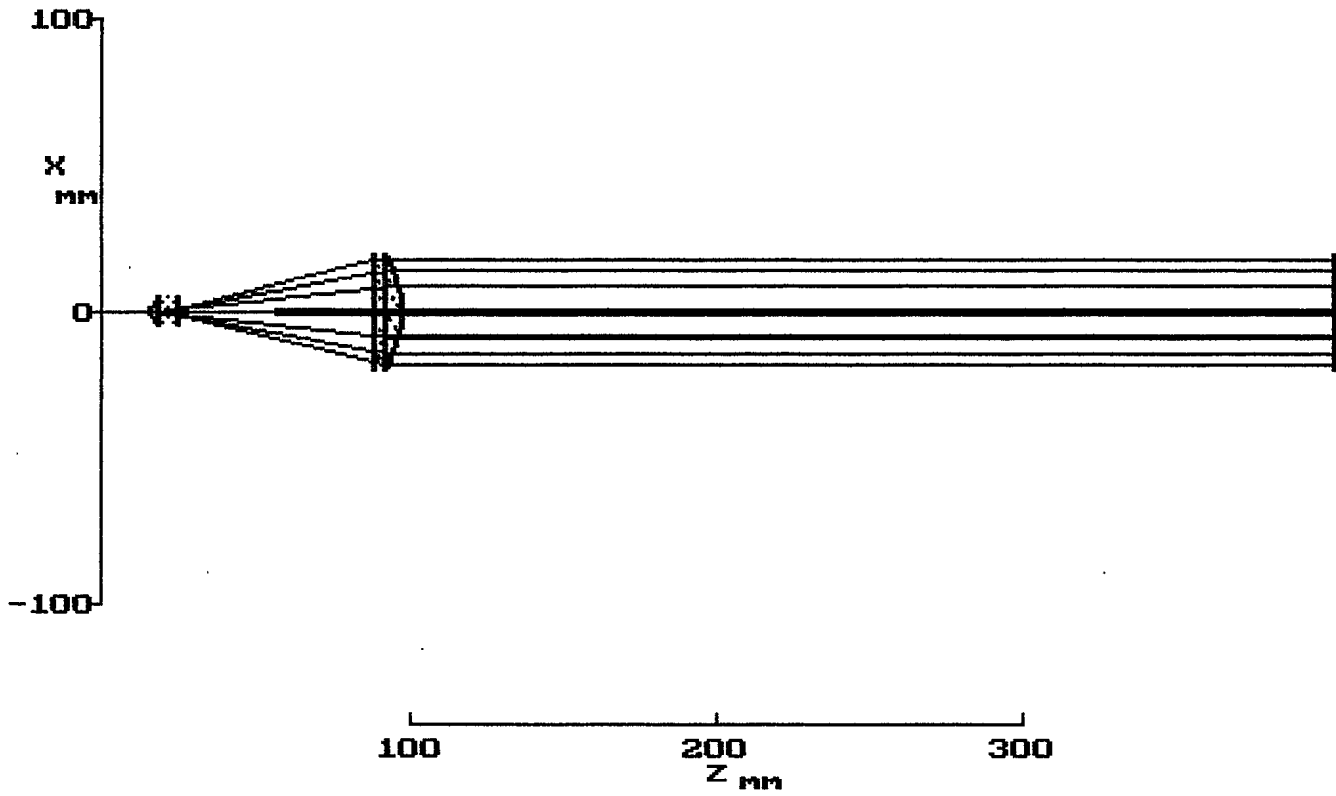


Figure 5. Outline of the beam-expander design, geometry #4

**Spot diagram of line generated by 1-D telescope
(z = 400 mm)**

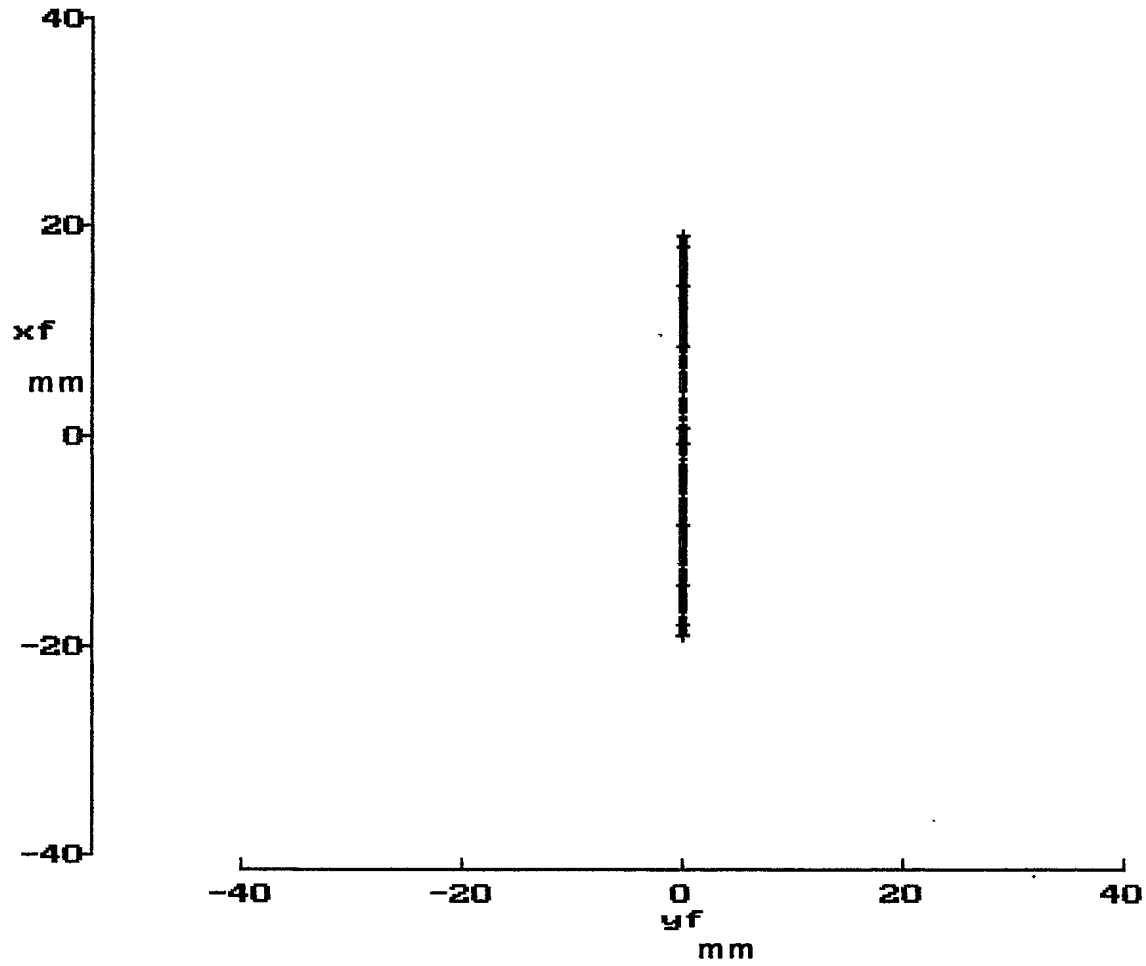
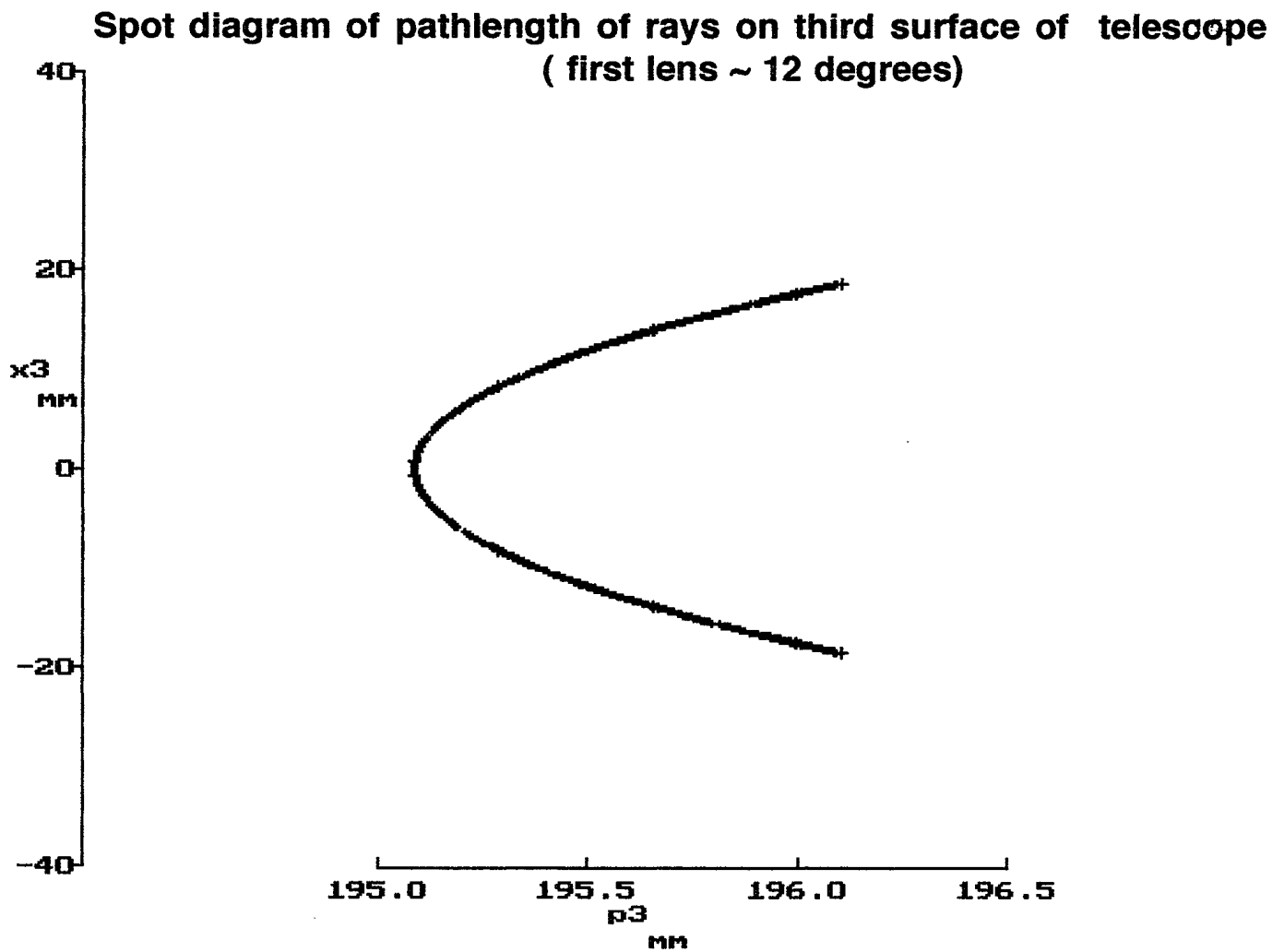


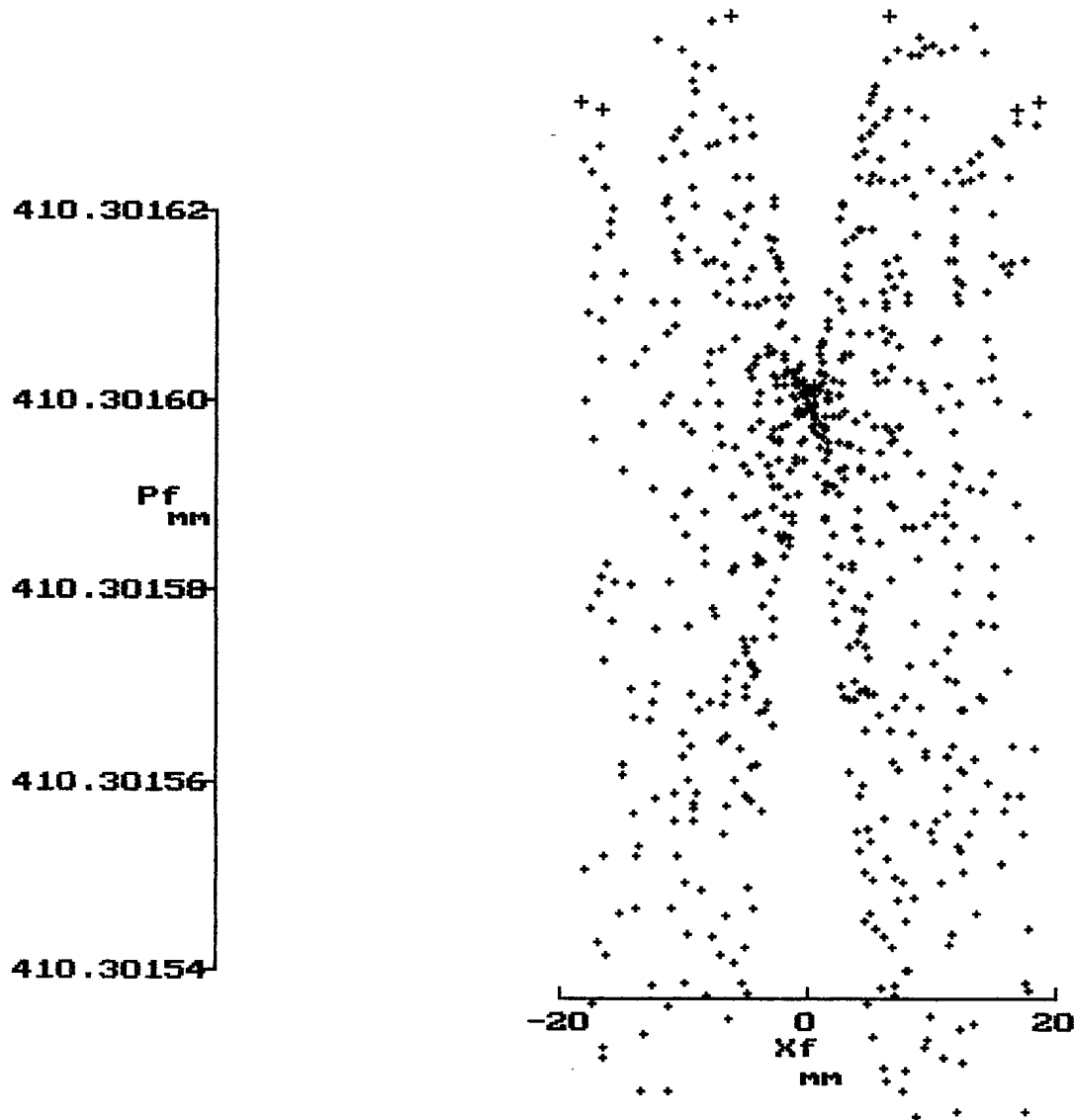
Figure 6. Spot diagram of line generated by 1-D telescope (1000 rays)



Wavefront flatness $\sim 10^4 \lambda$

Figure 7. Spot diagram of pathlength of 1000 rays on third surface (geometry #2)

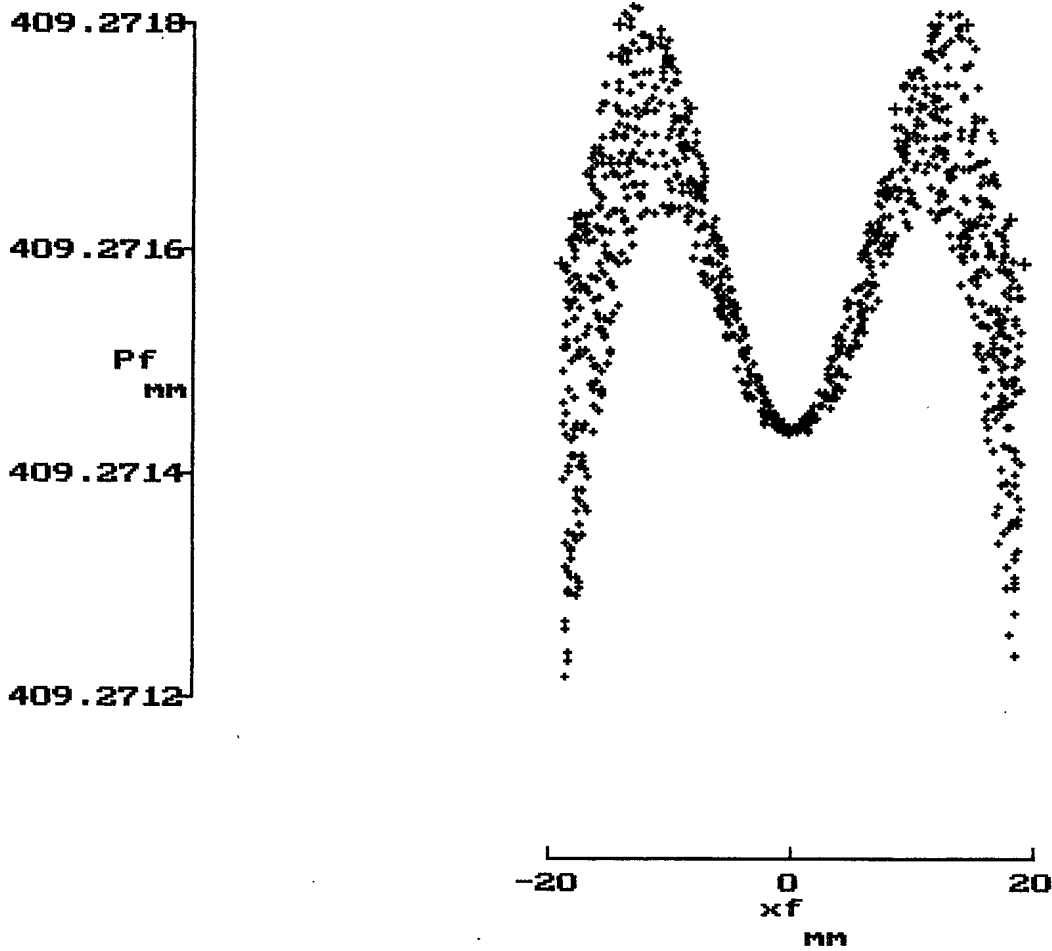
Spot diagram of pathlength of rays
(first lens ~ 6 degrees)



Wavefront flatness $\sim .5 \lambda$

Figure 8. Spot diagram of pathlength of 1000 rays at $z = 400$ mm (geometry #1)

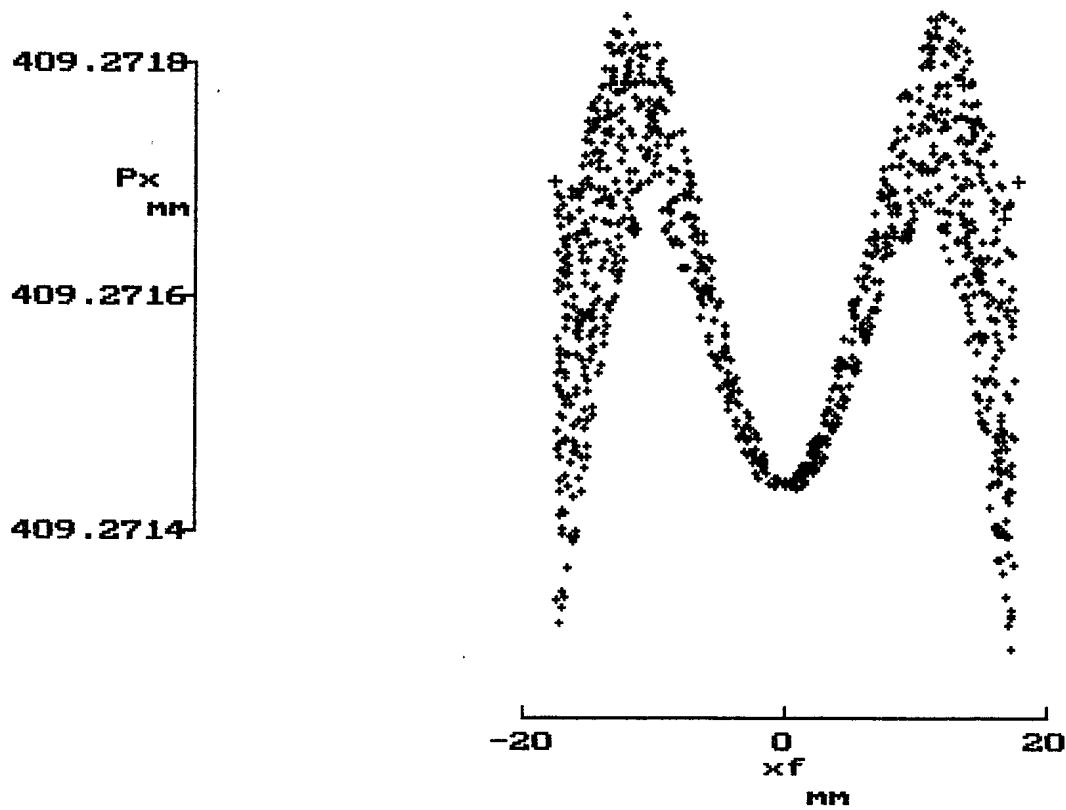
Spot diagram of pathlength of rays
(first lens ~ 12 degrees, long geometry)



Wavefront flatness $\sim .8 \lambda$

Figure 9. Spot diagram of pathlength of 1000 rays at $z = 400$ mm (geometry #2)

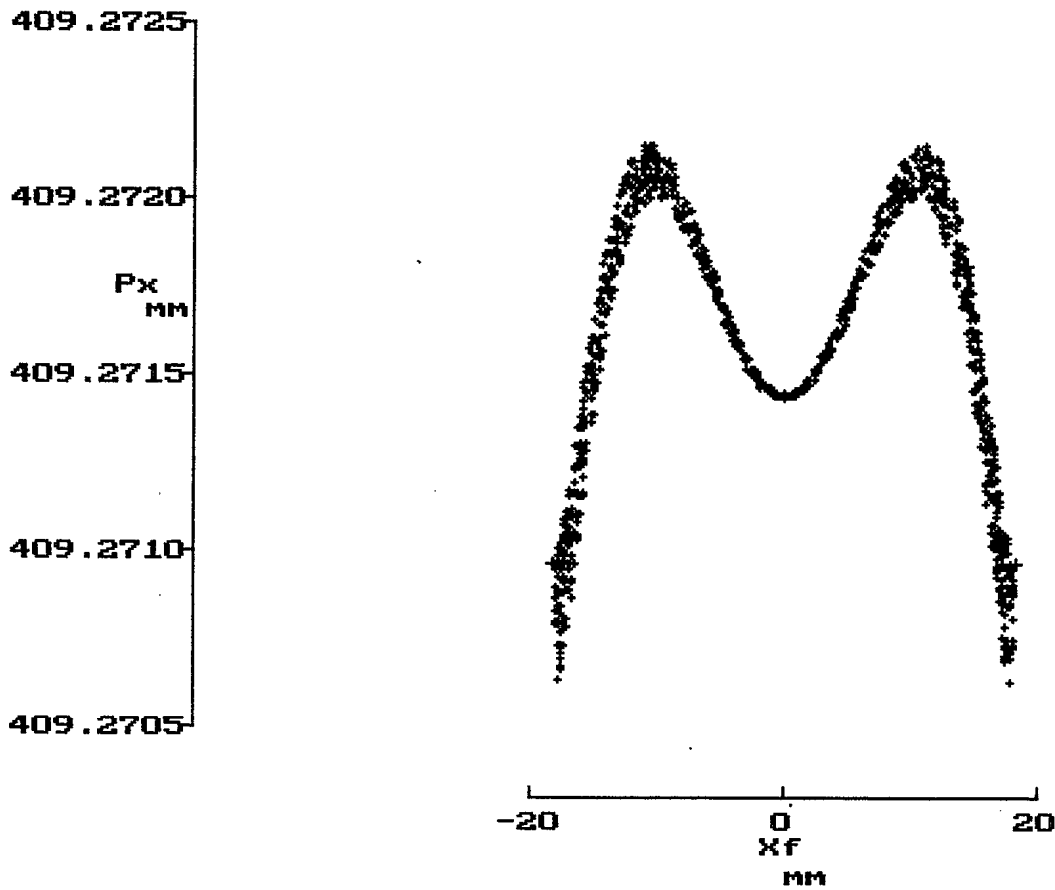
Spot diagram of pathlength of rays
(first lens ~12 degrees)



Wavefront flatness $\sim 1 \lambda$

Figure 10. Spot diagram of pathlength of 1000 rays at $z = 400$ mm (geometry #3)

Spot diagram of pathlength of rays
(first lens ~30 degrees)



Wavefront flatness $\sim 2.5 \lambda$

Figure 11. Spot diagram of pathlength of 1000 rays at $z = 400$ mm (geometry #4)

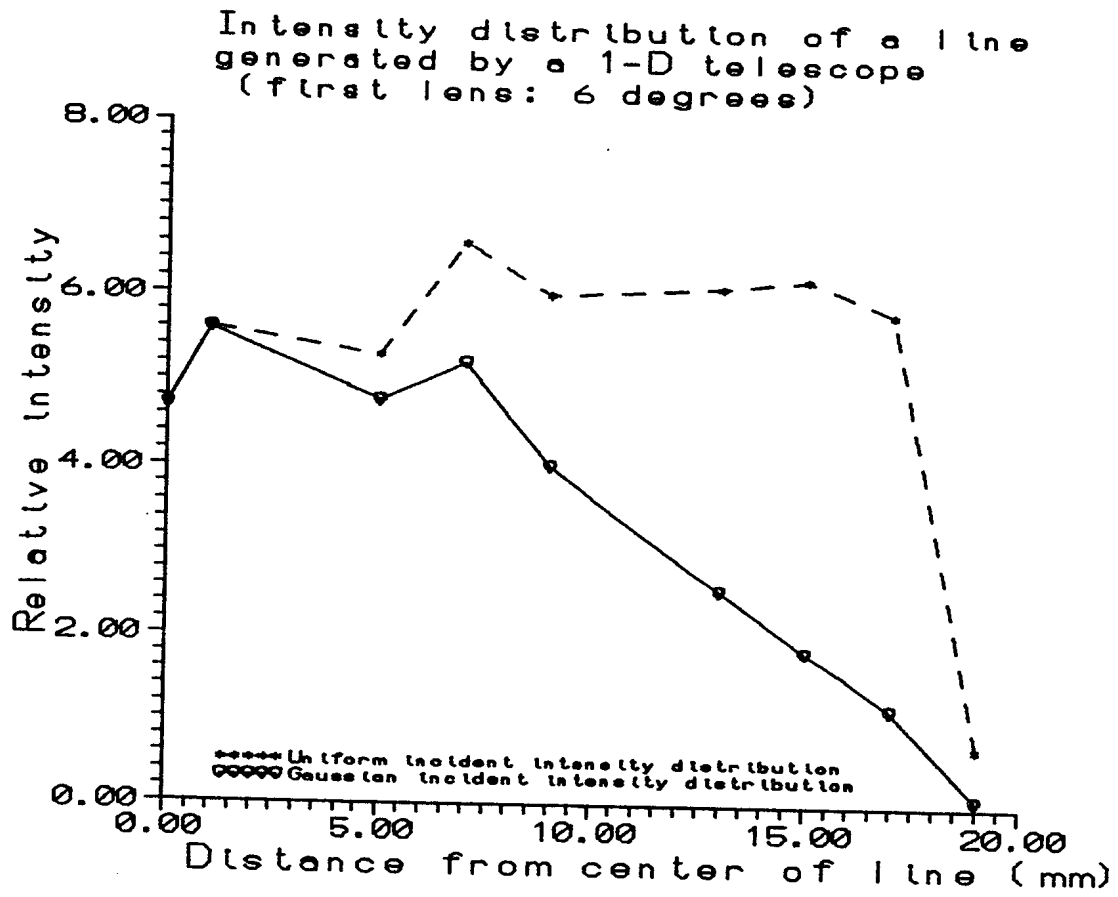


Figure 12. Intensity distribution at the observation plane (geometry #1)

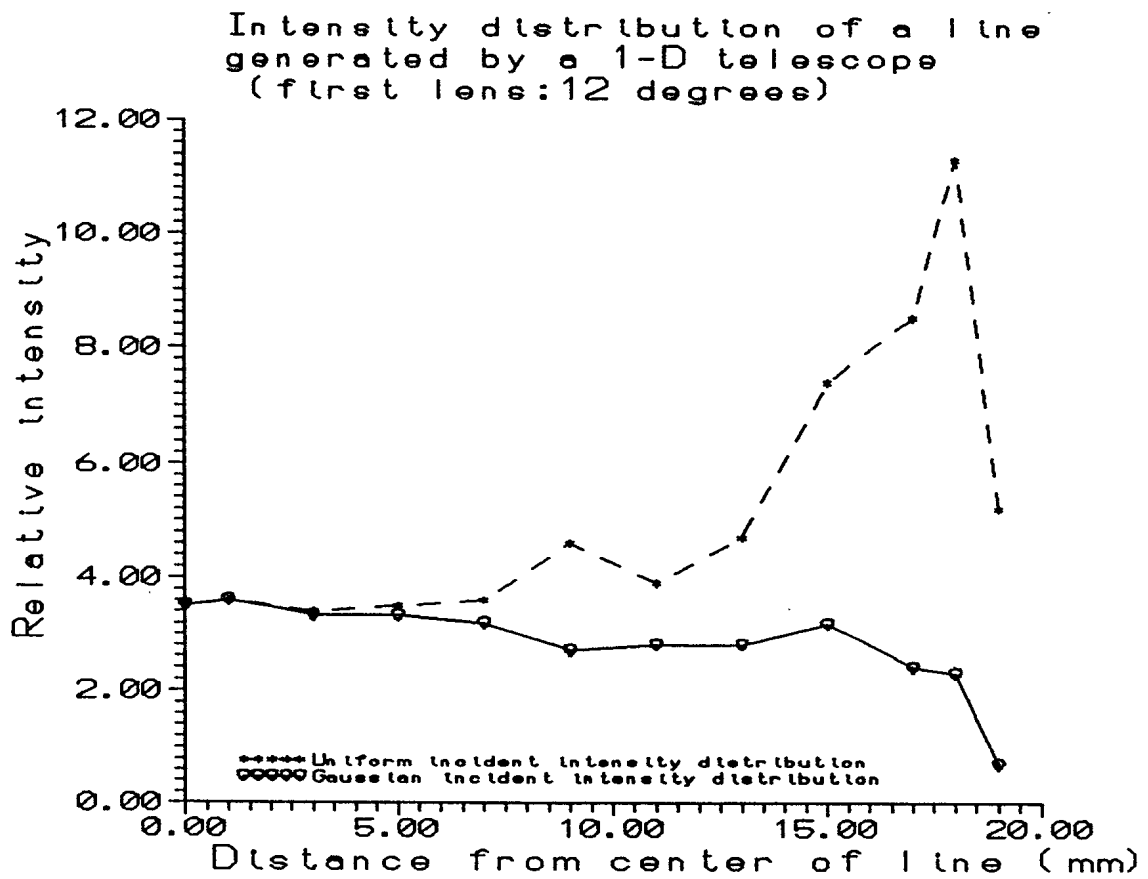


Figure 13. Intensity distribution at the observation plane (geometry #2)

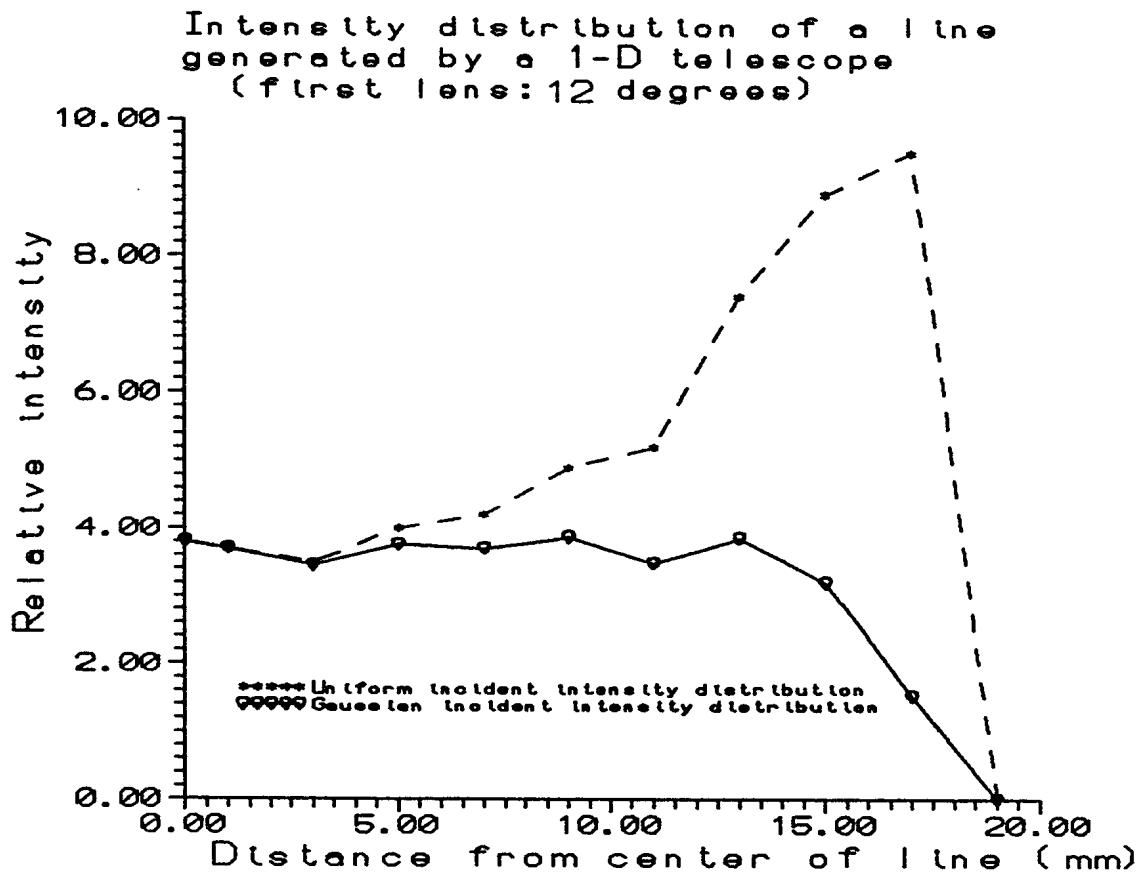


Figure 14. Intensity distribution at the observation plane (geometry #3)

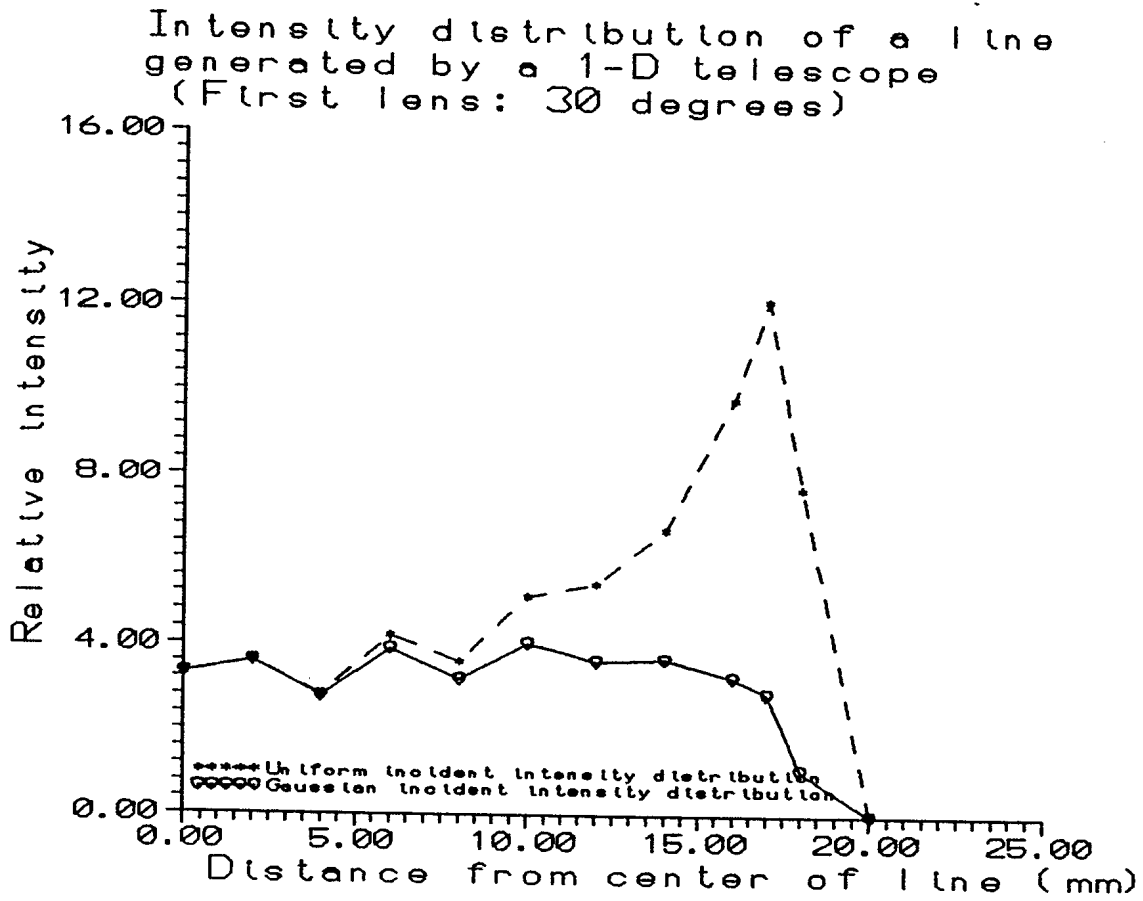


Figure 15. Intensity distribution at the observation plane (geometry #4)

1.3 Characteristics of the best design

It has been shown that the best design, regarding the wavefront flatness and the uniformity of the intensity distribution, is the one following geometry #2. We will now study the profile of the lenses in the beam-expander #2.

The cylindrical surface of an aspherical lens can be represented by the following equation:

$$z = \frac{cx^2}{1 + [1-(1+Q) c^2x^2]^{1/2}} \quad (1)$$

where $c = 1/R =$ inverse radius, and $Q =$ conic constant.

The profile of the conic surface of the Powell lens (first lens of the beam expander of geometry #2) is shown on figure 16 with the solid line. It can be seen that when we go far from the center of the surface ($x = 0$) the profile becomes almost linear. It can be shown that when

$$x \gg R$$

we get the following linear equation:

$$z \cong [-(1+Q)]^{-1/2} x + \left(\frac{R}{1+Q}\right) \quad (2)$$

which corresponds to a prislake profile as shown on figure 16 with the dashed lines.

Figure 17 shows the profile of the correcting lens and it is apparent that since the Q factor has an absolute value near zero the profile does not become linear as X increases. Instead of being a conic, the surface profile follows a prolate ellipsoid.

In theory the beam-expander based on geometry #2 should produce a collimated line of 37 mm, with 82% of the laser output energy confined in a length of 35 mm. In practice, if AR coatings are applied on each surface of the lenses, more than 75% of the laser energy should be confined in the useful part of the expanded beam. If we are to fabricate the beam-expander, there will be no problem in shaping the first lens since we know a useful production technique. But shaping the correcting lens will be a challenge, since it will require different tooling and polishing methods.

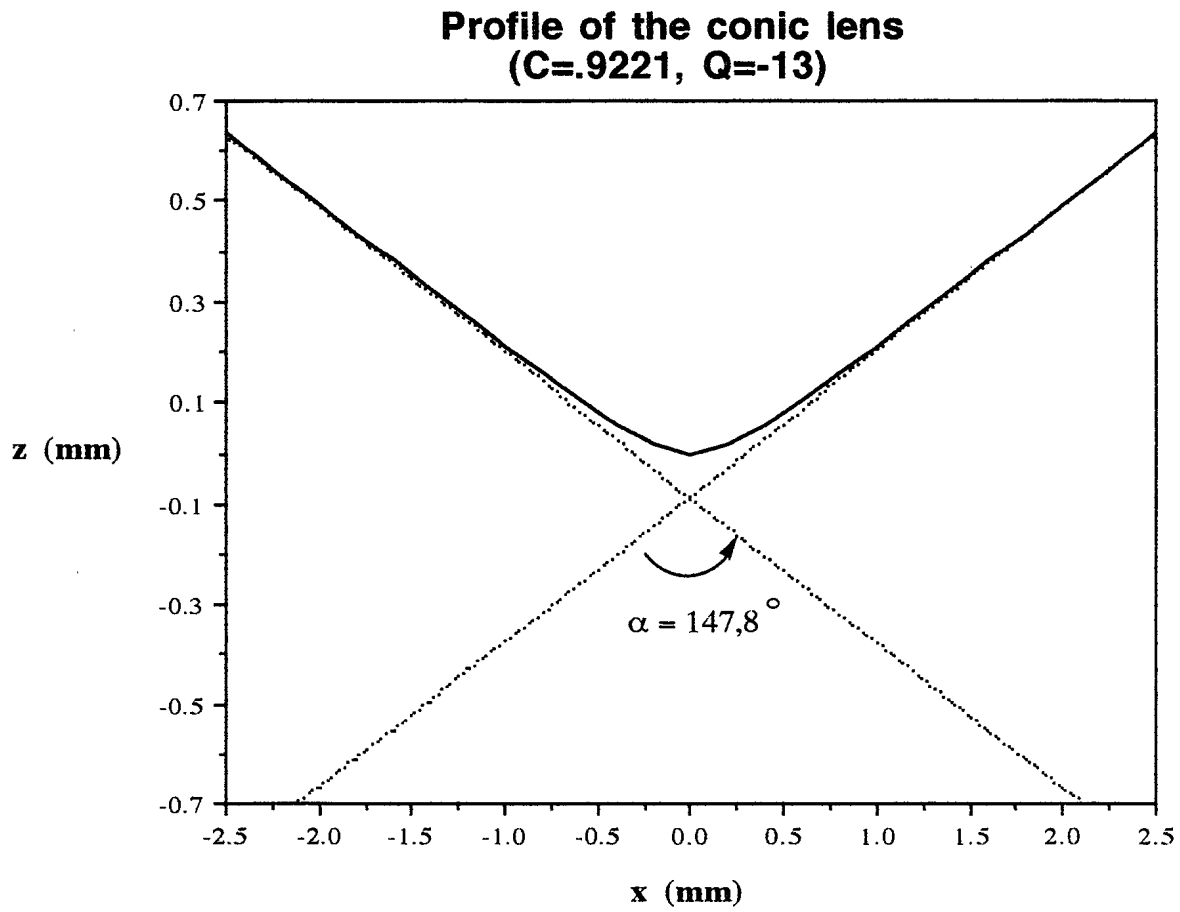


Figure 16. Profile of the Powell lens of geometry #2 according to equation (1)

**Profile of the aspherical lens
(C= -.011, Q= -.22)**

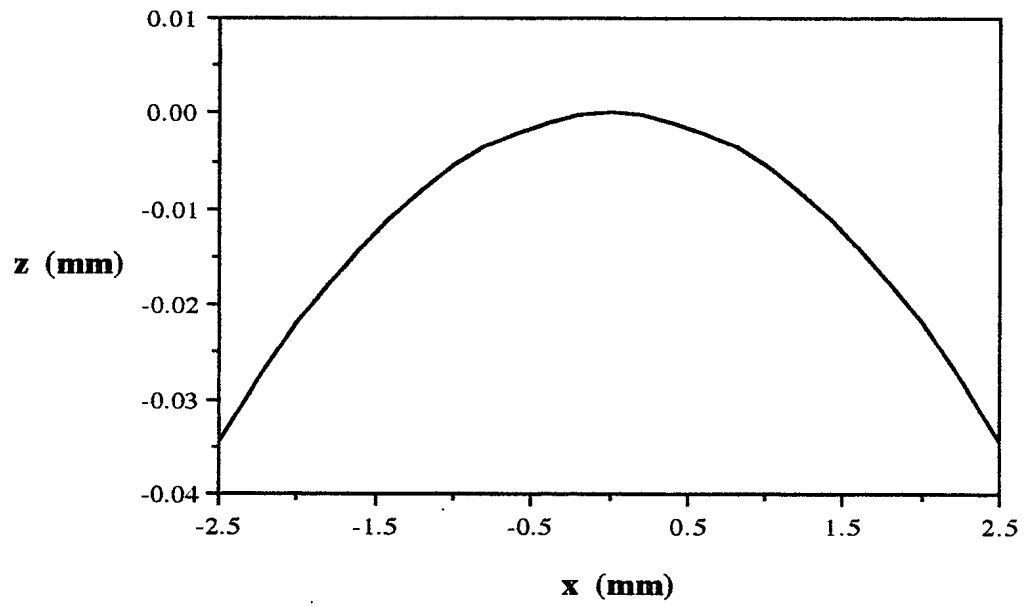


Figure 17. Profile of the correcting lens of geometry #2

2. DESIGN OF AN ANAMORPHIC BEAM-EXPANDER BASED ON A HOLOGRAPHIC OPTICAL ELEMENT (HOE)

2.1 *In-line geometry*

The simplest geometry one can imagine for recording and reconstructing a HOE is certainly an in-line geometry, as shown in figure 18, but it is not necessarily the most performing one. In our case, the HOE would be a correcting element to be used after the Powell lens in order to collimate the emerging beam and uniformize its wavefront. At the recording stage of the HOE, the reference beam would have to be similar to the beam emerging from the Powell lens to correct, and the object beam would have to be identical to the desired resulting beam, with a uniform intensity distribution and a flat wavefront. During reconstruction, or utilization of the HOE, a reconstruction beam (identical to the reference beam during recording) will be diffracted by the HOE and will give rise to the desired collimated beam.

The main problem with the in-line geometry is that the diffracted and the transmitted beams will be superimposed and that there will be no way to separate the flat wavefront from the aberrated one. Moreover, this geometry carries the problem of the "twins images": a real conjugate image of the object beam will be superimposed on the virtual image of the object beam. Since the object beam is a parallel beam, this problem will be less important than in the case of a complex object image, but the flatness of the wavefront at a given position Z will be diminished. Furthermore, in the in-line geometry, the maximum theoretical diffraction efficiency attainable is of ~33% for a thin transmission grating recorded in a phase medium.

The equation describing the thin grating behavior being:

$$d \sin \theta_m = m \lambda \quad (1)$$

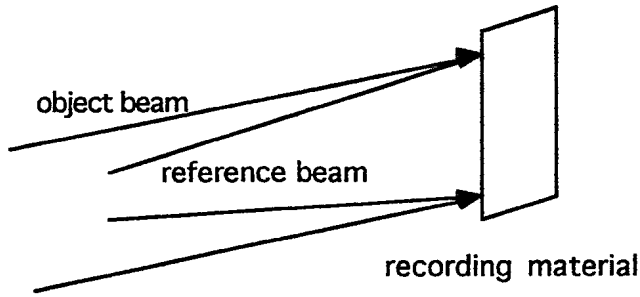
where d = grating period, θ_m = diffraction angle of the m^{th} order, m = order of diffraction and λ = wavelength, it is evident that the period will be extremely large for a geometry where the diffraction angle is practically null. This will prevent the grating from behaving like a thick one as long as the thickness of the recording material is finite. Unfortunately, for the diffraction efficiency to be maximized and for the grating to work in the "volume" regime, the thickness of the HOE would have to be infinite in order for the Q factor of the grating to be $\gg 10$, as stated by the following "thickness criterium" equation:

$$Q = 2 \pi \lambda_0 t / n_0 d^2 \gg 10 \quad (2)$$

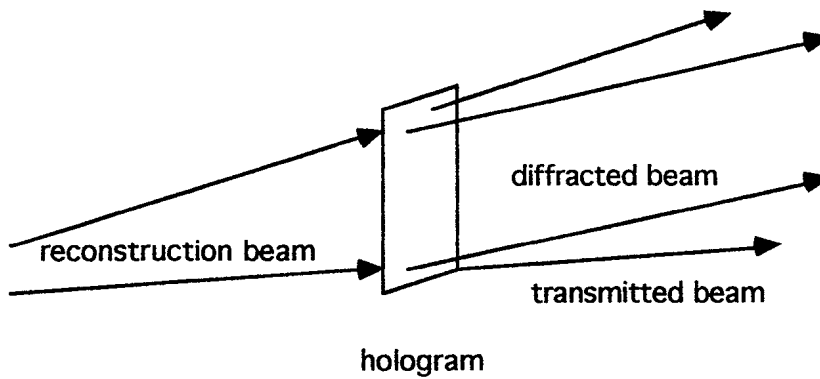
where t = thickness of the material and n_0 = refractive index of the material.

In conclusion the in-line geometry is inapplicable since it is impossible to obtain high diffraction efficiencies and non-overlapping beams.

In-Line geometry



a. recording



b. reconstruction

Figure 18. In-line geometry for recording and reconstructing a HOE capable of correcting the beam emerging from a Powell lens

2.2 Off-axis geometry

In order to increase the maximum diffraction efficiency attainable by the HOE, it is necessary to adopt the off-axis geometry shown in figure 19. The HOE will certainly be less practical to use than with the in-line geometry, but the diffracted and transmitted beams will no longer overlap during reconstruction. In theory it would then be possible to isolate the diffracted beam and use it to illuminate a Bragg cell.

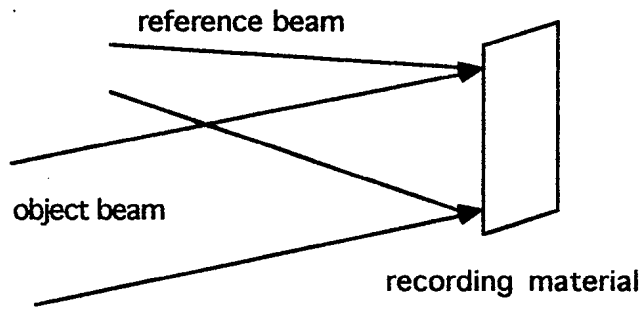
If, for example, commercial plates from Agfa Gaevert (nominal thickness of $7\ \mu\text{m}$) were used to record the HOE, the latter would have to be designed to be illuminated at $\sim 20^\circ$ from the normal for the Q factor criterium to be satisfied and for the maximum diffraction efficiency to raise around 60%. On the other hand, by using hand-made DCG plates of $\sim 25\ \mu\text{m}$, the HOE could be designed to be used at $\sim 10^\circ$ from the normal and still work in the "volume" regime. Unfortunately, the hand-made plates always present some thickness non-uniformities ($\sim \pm .4\ \mu\text{m}$ over a 35 mm length) that would inevitably distort the resulting wavefront.

Besides the "geometry difficulties" associated with the recording of HOEs, there is an intrinsic problem related to our case: for both the in-line and the off-axis geometries, the object beam must have the same characteristics as the desired resulting diffracted beam. Its intensity must not then vary more than $\pm 10\%$ over its length and its wavefront must have a flatness of $\lambda/10$! This is very difficult to obtain with ordinary optics and in order to achieve this with a cylindrical lens, we would have to use a very small central portion of the gaussian beam. Thus more than 80% of the laser output energy would be lost and the exposure times for recording the HOE would be extremely long! The recording process would become very time-consuming and problems of instability would then lower significantly the maximum diffraction efficiency attainable.

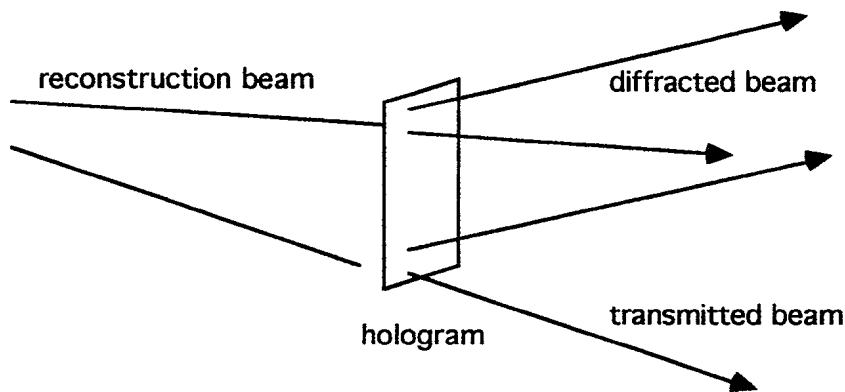
Moreover, another difficulty lies in the development process of the HOE. In general, the amplification occurring during the development is not rigorously linear, and consequently some noise and distortion of the recorded fringes can appear and prevent the diffracted wavefront from being the exact replica of the recorded object wavefront.

For all the reasons discussed above, it would be very difficult to produce a HOE that would correct satisfactorily the beam exiting from a Powell lens.

Off-axis geometry



a. recording



b. reconstruction

Figure 19. Off-axis geometry for recording and reconstructing a HOE capable of correcting the beam emerging from a Powell lens

3. DESIGN OF AN ANAMORPHIC BEAM-EXPANDER BASED ON A DIFFRACTIVE ELEMENT

Diffractive optics refers to the technology of producing surface-relief computer-generated diffractive patterns directly onto an optical material. Computer-generated diffractive surfaces offer a very flexible means of controlling and shaping phase fronts or bending rays. With diffractive optics it is possible to modify the phase of an incoming gaussian beam and perform an intensity transformation and a focusing operation with a single element. On the negative side diffractive surfaces introduce strong chromatic aberrations and diffract less than 100% of the incoming energy to the desired order. Moreover, manufacturing processes are still relatively expensive.

Figure 20 shows how a diffractive element could be used to correct the beam emerging from a Powell lens (off-axis geometry).

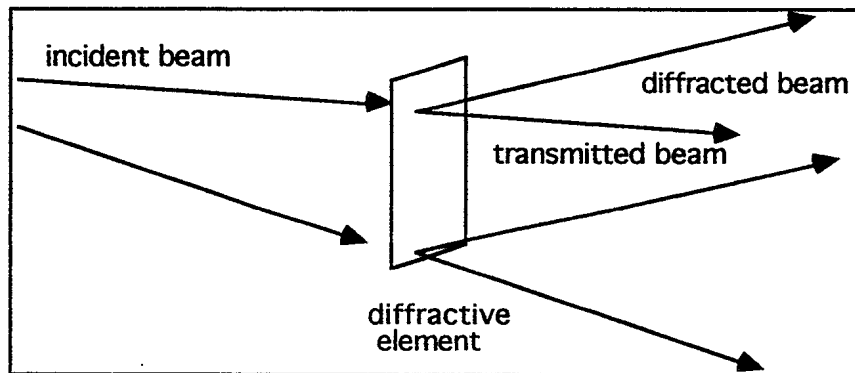


Figure 20. Geometry for using a diffractive element to correct the beam emerging from a Powell lens

To be able to use diffractive optics to uniformize a certain wavefront, we must know exactly (in a mathematical form) the shape of the wavefront arriving at the entrance plane of the diffractive element. This information is essential for the calculation of the required surface profile of the element. Since the lens that created the wavefront in the first place is not an ideal lens, it has imperfections over its surfaces, and a set of manufactured lenses of the same nominal curvature will always show some differences. So, to be corrected by a diffractive element, the wavefront exiting each lens would have to be mapped in order for the diffractive element profile to be calculated.

For a binary diffractive element the maximum diffraction efficiency attainable is about 40%. In order to separate the first and zeroth orders, the distance between the diffractive element and the

plane of location of the desired wavefront would have to be quite large (~1.6 m), since the minimum period of such a binary element would be about $25 \mu\text{m}$ with the current technology.

To be more efficient the diffractive element must have a multilevel profile. Unfortunately, the multilevel technology is not yet a commercially viable alternative, the fabrication costs of a single element being in the 50 000 dollars range. However, this is a promising technology that could eventually represent an interesting and cost-effective way to implement the wavefront correction required.

4. SELECTION OF THE BEST DESIGN

In conclusion, it appears that the best way of accomplishing the wavefront transformation of a line generated by a conic lens is **by the addition of another aspherical lens:**

- the energy loss is minimized compared to the two other methods
- the in-line geometry is possible
- the design and calculations are relatively simple
- the costs are lower than for the two other methods.

We are submitting these comments to the Scientific Authority for review and discussion. A specific approach will be selected by the Scientific Authority to be implemented during Phase 2 of this contract.

SECURITY CLASSIFICATION OF FORM
(highest classification of Title, Abstract, Keywords)

DOCUMENT CONTROL DATA

(Security classification of title, body of abstract and indexing annotation must be entered when the overall document is classified)

<p>1. ORIGINATOR (the name and address of the organization preparing the document. Organizations for whom the document was prepared, e.g. Establishment sponsoring a contractor's report, or tasking agency, are entered in section 8.) DEFENCE RESEARCH ESTABLISHMENT OTTAWA NATIONAL DEFENCE SHIRLEY BAY, OTTAWA, ONTARIO K1A 0K2 CANADA</p>	<p>2. SECURITY CLASSIFICATION (overall security classification of the document, including special warning terms if applicable) UNCLASSIFIED</p>
--	--

3. TITLE (the complete document title as indicated on the title page. Its classification should be indicated by the appropriate abbreviation (S,C or U) in parentheses after the title.)
THE DESIGN, MANUFACTURE AND PACKAGING OF AN ANAMORPHIC BEAM-EXPANDER TO ILLUMINATE BRAGG CELLS IN A TIME-INTEGRATING CORRELATOR (U)

4. AUTHORS (Last name, first name, middle initial)
LASIRIS INC.

<p>5. DATE OF PUBLICATION (month and year of publication of document) 31 JANUARY 1993</p>	<p>6a. NO. OF PAGES (total containing information. Include Annexes, Appendices, etc.) 29</p>	<p>6b. NO. OF REFS (total cited in document) NIL</p>
---	--	--

7. DESCRIPTIVE NOTES (the category of the document, e.g. technical report, technical note or memorandum. If appropriate, enter the type of report, e.g. interim, progress, summary, annual or final. Give the inclusive dates when a specific reporting period is covered.)
CONTRACTOR REPORT

8. SPONSORING ACTIVITY (the name of the department project office or laboratory sponsoring the research and development. Include the address.)
DEFENCE RESEARCH ESTABLISHMENT OTTAWA
NATIONAL DEFENCE
SHIRLEY BAY, OTTAWA, ONTARIO K1A 0K2 CANADA

<p>9a. PROJECT OR GRANT NO. (if appropriate, the applicable research and development project or grant number under which the document was written. Please specify was project or grant)</p>	<p>9b. CONTRACT NO. (if appropriate, the applicable number under which the document was written) W7714-2-9654/01-ST</p>
--	--

<p>10a. ORIGINATOR'S DOCUMENT NUMBER (the official document number by which the document is identified by the originating activity. This number must be unique to this document.)</p>	<p>10b. OTHER DOCUMENT NOS. (Any other numbers which may be assigned this document either by the originator or by the sponsor)</p>
---	--

11. DOCUMENT AVAILABILITY ~~any~~ limitations on further dissemination of the document, other than those imposed by security classification)

- Unlimited distribution
- Distribution limited to ~~defence~~ departments and defence contractors; further distribution only as approved
- Distribution limited to ~~defence~~ departments and Canadian defence contractors; further distribution only as approved
- Distribution limited to ~~government~~ departments and agencies; further distribution only as approved
- Distribution limited to ~~defence~~ departments; further distribution only as approved
- Other (please specify):

12. DOCUMENT ANNOUNCEMENT (any limitation to the bibliographic announcement of this document. This will normally correspond to the Document Availability (11); ~~however~~, where further distribution (beyond the audience specified in 11) is possible, a wider announcement audience may be ~~selected~~.)

13. ABSTRACT (a brief and factual summary of the document. It may also appear elsewhere in the body of the document itself. It is highly desirable that the abstract of classified documents be unclassified. Each paragraph of the abstract shall begin with an indication of the security classification of the information in the paragraph (unless the document itself is unclassified) represented as (S), (C), or (U). It is not necessary to include here abstracts in both official languages unless the text is bilingual).

(U) The purpose of this project is to design and produce an anamorphic beam-expander to illuminate Bragg cells in a time-integrating correlator. The basic element of the beam-expander is a "Powell lens (designed in 1987 by Ian Powell from the National Council of Research Canada) which is a spherical element capable of producing a beam with a uniform intensity diverging in one dimension on the X axis. On the other axis, Y, the size of the beam is determined only by the divergence of the laser beam. Unfortunately, the wavefront is not flat because of the presence of aberrations introduced by the lens itself. The goal is to design and manufacture an element which would collimate the diverging beam exiting from a Powell lens, and correct the wavefront in order to obtain the best flatness possible, while still retaining the uniform intensity, on the X axis, of the beam.

(U) The project is separated in two phases: Phase 1 where the design and calculation of an anamorphic beam-expander based on three different elements are performed, and Phase 2 where the prototype beam-expander is manufactured and packaged according to the selected design.

(U) This preliminary report illustrates the work done under Phase 1 and is divided in four chapters describing respectively:

1. Correction of the wavefront emerging from a Powell lens by a spherical lens
2. Correction of the wavefront emerging from a Powell lens by a holographic optical element (HOE)
3. Correction of the wavefront emerging from a Powell lens by a glass diffractive element
4. Selection of the best design.

14. KEYWORDS, DESCRIPTORS or IDENTIFIERS (technically meaningful terms or short phrases that characterize a document and could be helpful in cataloguing the document. They should be selected so that no security classification is required. Identifiers, such as equipment model designation, trade name, military project code name, geographic location may also be included. If possible keywords should be selected from a published thesaurus. e.g. Thesaurus of Engineering and Scientific Terms (TEST) and that thesaurus-identified. If it is not possible to select indexing terms which are Unclassified, the classification of each should be indicated as with the title.)

ANAMORPHIC LASER BEAM EXPANSION
LINE ILLUMINATION

UNCLASSIFIED

SECURITY CLASSIFICATION OF FORM

#148560

NO. OF COPIES NOMBRE DE COPIES	COPY NO. COPIE N°	INFORMATION SCIENTIST'S INITIALS INITIALES DE L'AGENT D'INFORMATION SCIENTIFIQUE
1	1	DAR
AQUISITION ROUTE FOURNI PAR	DREO	
DATE	23 NOVEMBER 1994	
DSIS ACCESSION NO. NUMÉRO DSIS	95-02736	

DND 1158 (6-87)



**PLEASE RETURN THIS DOCUMENT
TO THE FOLLOWING ADDRESS:**
 DIRECTOR
 SCIENTIFIC INFORMATION SERVICES
 NATIONAL DEFENCE
 HEADQUARTERS
 OTTAWA, ONT. - CANADA K1A 0K2

**PRIÈRE DE RETOURNER CE DOCUMENT
À L'ADRESSE SUIVANTE:**
 DIRECTEUR
 SERVICES D'INFORMATION SCIENTIFIQUES
 QUARTIER GÉNÉRAL
 DE LA DÉFENSE NATIONALE
 OTTAWA, ONT. - CANADA K1A 0K2